Head-tail Modes for the Strong Space Charge Gaussian Beam

Timofey Zolkin

The University of Chicago, Department of Physics

zolkin@uchicago.edu

Jan 26, 2015

Overview

1. Design of Digital Filter for FNAL Booster Damper

The FNAL Booster accelerator is a proton synchrotron, originally designed and constructed in the beginning of 1970's to match the beam from the linear accelerator to the Fermilab Main Ring.

(a.), (b.) Satellite images of the Fermilab site showing Linear Accelerator (LINAC), Booster, Main Injector (MI), Recycler (R) and Tevatron ring. (c.) Photo of the Fermilab Willson Hall, LINAC and Booster.

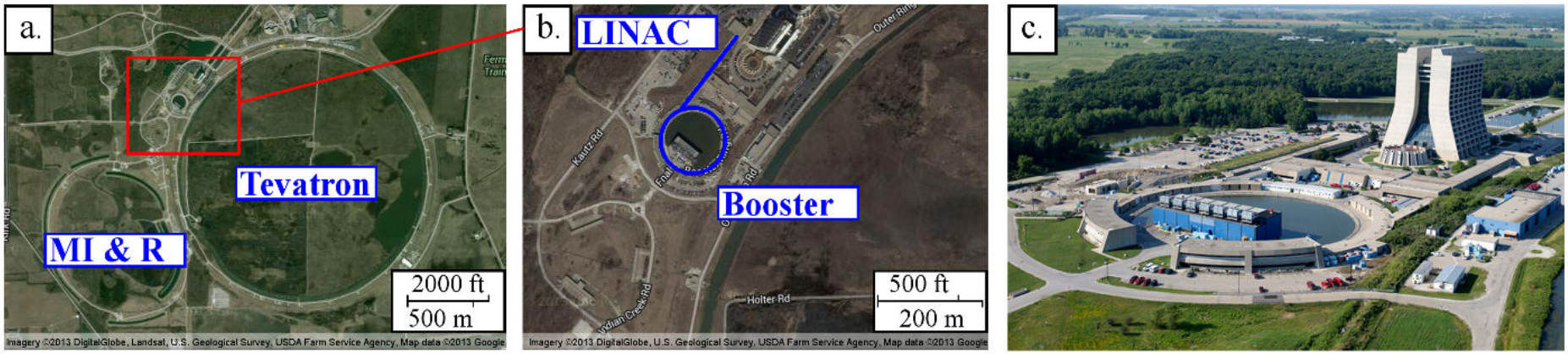

Brief facts

Since the 70's the whole accelerator complex has undergone many changes. At the present time, Booster accumulates the 400 MeV proton beam from the LINAC and then gives an intermediate boost to the beam energy. Booster was build as a fast cycling machine operating at 15 Hz which goes through repeated acceleration cycles delivering extracted 8 GeV beam pulses (referred to as a batch) to different experiments or filling the Main Injector ring which is about seven times larger.

A multiple turn injection system increases the Booster intensity; it allows to stack successive turns of LINAC beam layered on top of each other. LINAC provides Booster with 400 MeV debunched H^- ion beam. The H^- ions and circulating beam passes through the stripping foil, which removes electrons of the ions and made of a thin layer of carbons. Operationally, the practical limit for maximum intensity is about 7 to 8 turns; fractional turns are not used normally.

Linear model of transverse motion (Hill's equation)

$$\mathcal{K}_0[p_x, p_z, x, z; s] = \sum_{q=x,z} \left[\frac{p_q^2}{2} + g_q(s) \frac{q^2}{2} \right]$$

$$q(s) = \sqrt{2 J_q \beta_q(s)} \cos\left[\psi_q(s) + \delta_q\right]$$

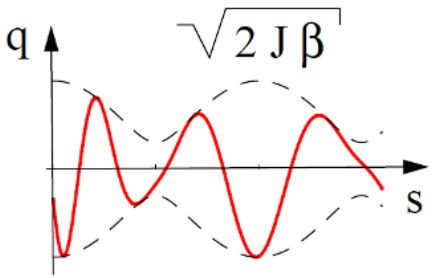

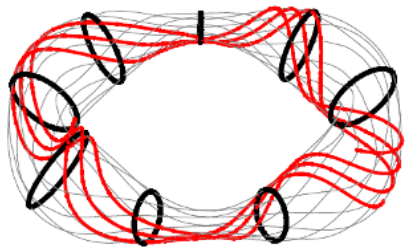

Booster lattice consists of 96 combined function magnets which are arranged in 24 superperiods

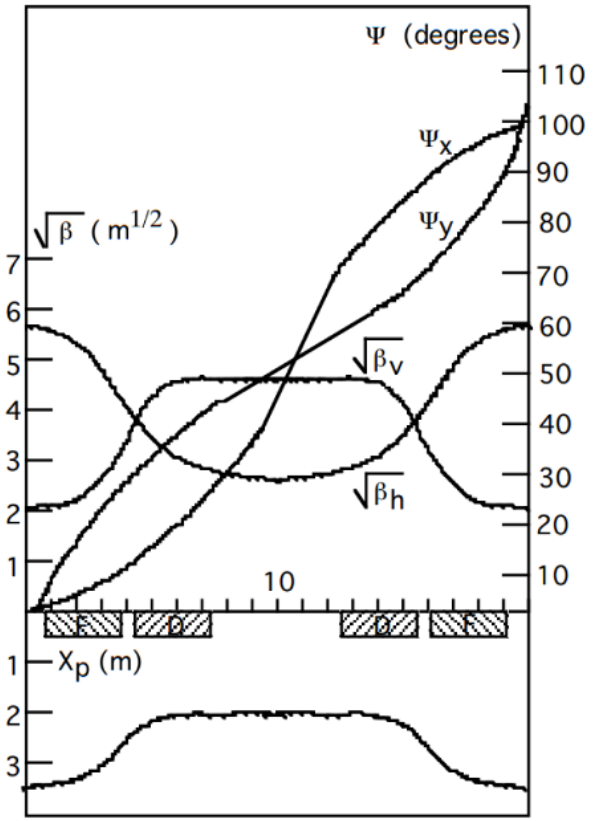

The most common method of a non-intercepting particle beam monitoring is to couple to the electromagnetic field of the beam. Conventional pickup is a pair of electrodes on which signals are induced.

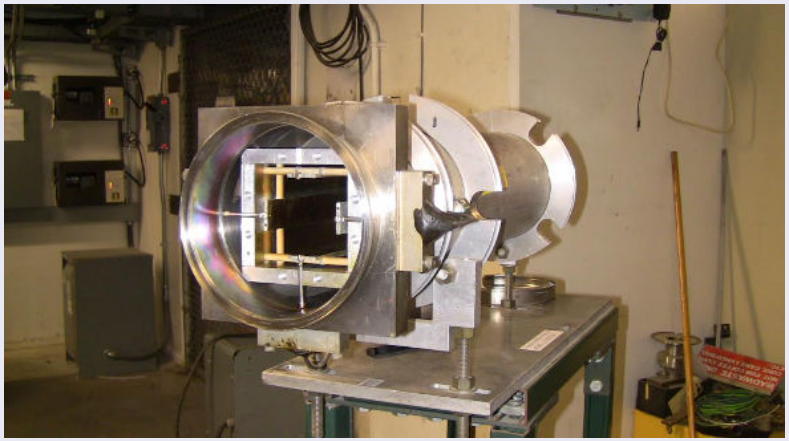

Beam position $q \propto \frac{Left - Right}{Left + Right} = \frac{\Delta}{\Sigma}$

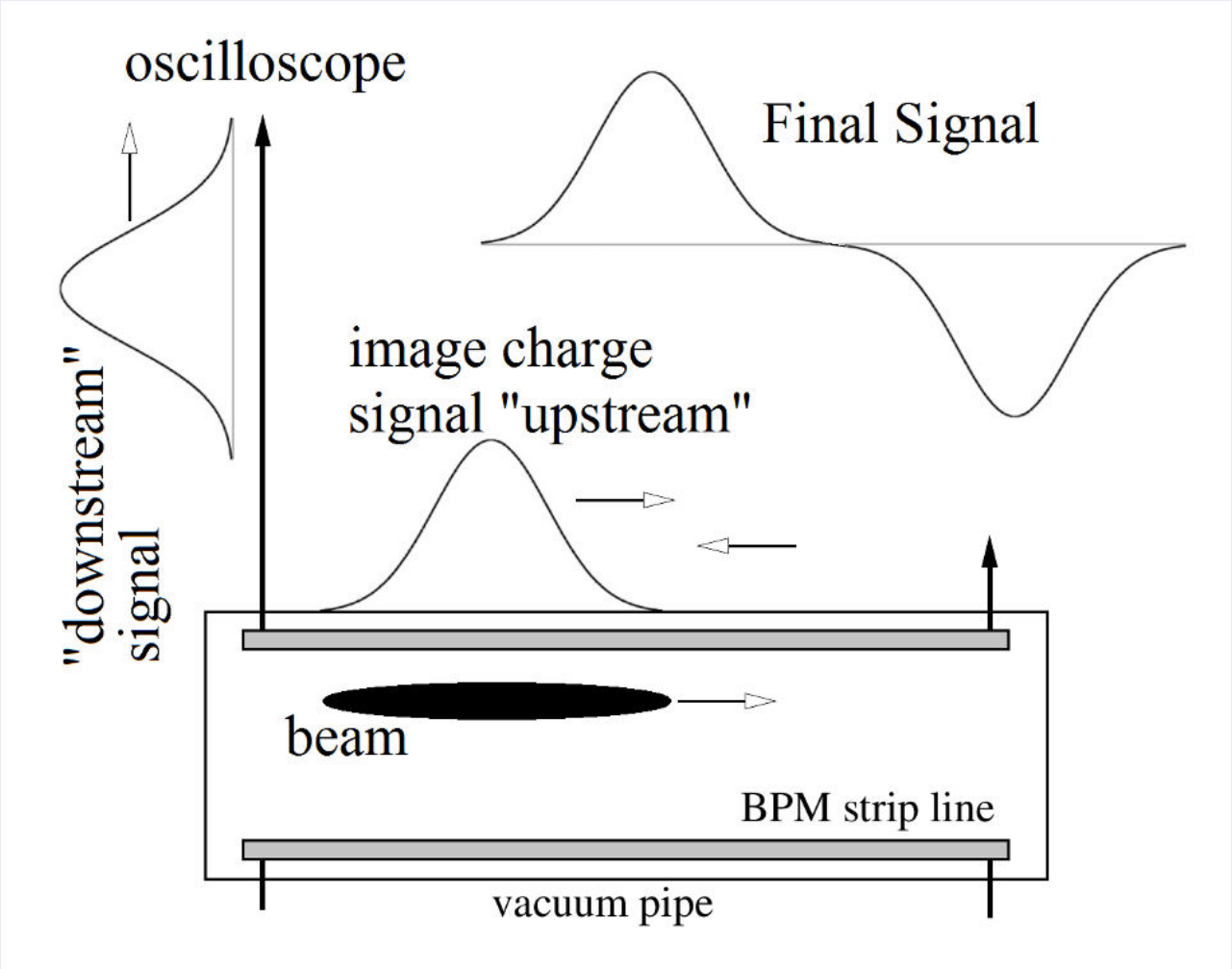

Existing problems:

- Beam equilibrium orbit is offset geometrical center of BPM
- Beam orbit undergoes rapid radial displacement in order to save a beam during transition

Signals from horizontal and vertical plates of BPM

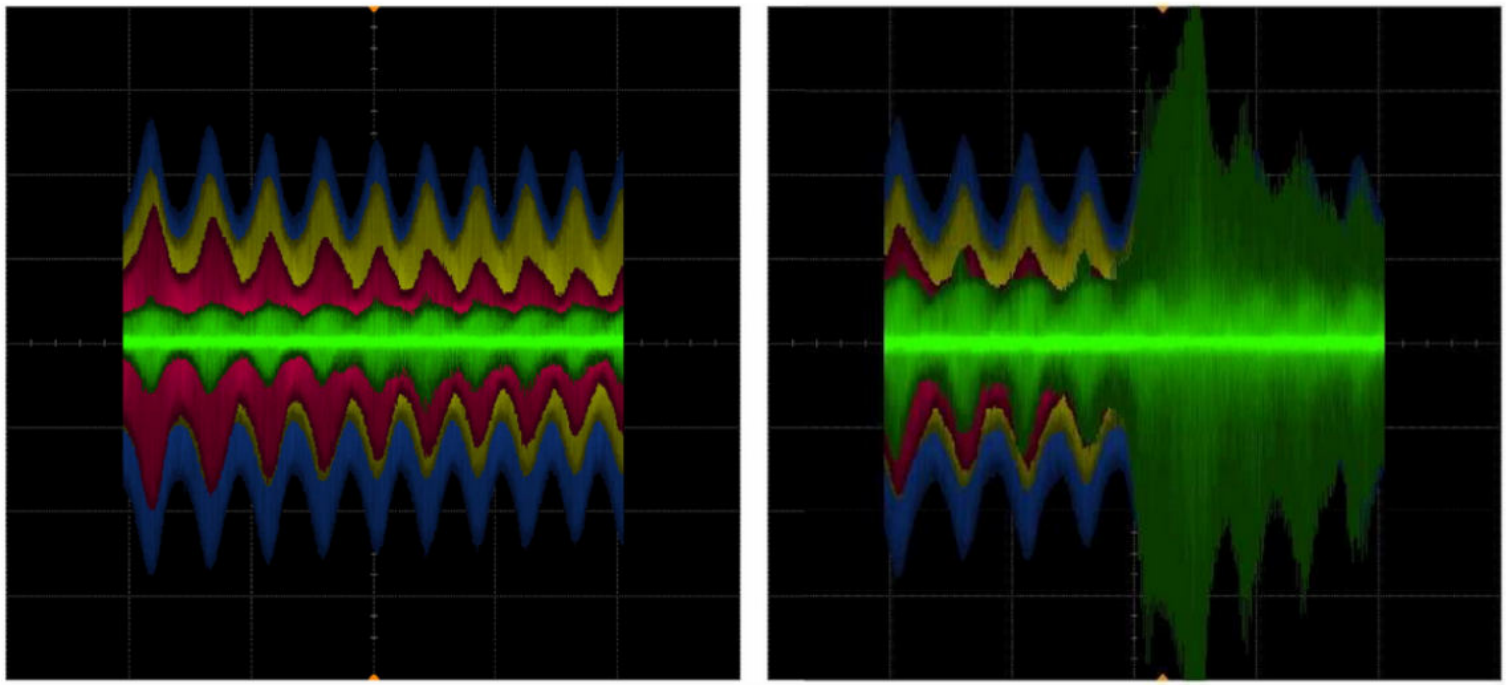

Stable cycle (Np=4 turns) **Instability (Np=12 turns)**

Theoretical description of head-tail modes for strong space charge beam was developed by Alexy Burov in 2009.

A. Burov, **"Head-tail modes for strong space charge"**, *Phys. Rev. ST Accel. Beams* 12(4), 044202, 2009.

Theory is valid when the space charge tune shift in the 3D center of the bunch is much larger than both the synchrotron tune, Q_s, and the wake driven coherent tune shift, Q_w:

$$\boxed{Q_{\max} \gg Q_s, Q_w}\,.$$

Single-particle equation of motion (rigid-slice approximation)

Force due to a space charge is $\propto$ to particle offset from local beam centroid

$$\dot{x}_i(\theta) = iQ\left[\tau_i(\theta)\right]\left\{x_i(\theta) - \bar{x}\left[\theta, \tau_i(\theta)\right]\right\} - i\zeta v_i(\theta) x_i(\theta)$$

where $x_i(\theta)$ is a slow variable related to the betatron offset of the i-th particle, $X_i(\theta) = x_i(\theta)e^{-iQ_b\theta}$, and, $\bar{X}(\theta, \tau)$ is an offset of the beam slice.

- θ — time in radians, $\dot{(\ldots)} \stackrel{\text{def}}{=} \mathrm{d}/\mathrm{d}\,\theta$,
- τ — distance along the bunch in radians,
- Q_b — betatron frequency,
- $Q(\tau)$ — space charge tune shift,
- $v_i \stackrel{\text{def}}{=} \dot{\tau}_i(\theta)$ — velocity of i-th particle,
- $\zeta = -\xi/\eta$ — effective chromaticity; $\xi = \frac{\mathrm{d}\,Q_b}{\mathrm{d}\Delta p/p}$ and $\eta = \frac{1}{\gamma_t^2} - \frac{1}{\gamma^2}$ are conventional chromaticity and slippage factor respectively.

Step 1. Chromaticity exclusion, $x_i(\theta) = y_i(\theta)e^{-i\zeta\tau_i(\theta)}$.

$$\dot{y}_i(\theta) = iQ\left[\tau_i(\theta)\right]\left\{y_i(\theta) - \bar{y}\left[\theta, \tau_i(\theta)\right]\right\}.$$

Step 2. 2nd order ODE for strong space charge eigenfunctions.

$$\boxed{\frac{\mathrm{d}}{\mathrm{d}\tau}\left(u^2(\tau)\frac{\mathrm{d}\bar{y}(\tau)}{\mathrm{d}\tau}\right) + \nu Q\bar{y}(\tau) = 0},$$

with

$$u^2(\tau) = \frac{\int_{-\infty}^{\infty} v^2 f(v,\tau)\,\mathrm{d}v}{\int_{-\infty}^{\infty} f(v,\tau)\,\mathrm{d}v}.$$

Step 3. Natural system of units.

- τ is measured in units of the rms bunch length σ,
- ν_k is measured in units of $\dfrac{u^2}{\sigma^2 Q_{\mathrm{eff}}(0)} = \dfrac{Q_s^2}{Q_{\mathrm{eff}}(0)}$.

2.1 Head-Tail Modes for Gaussian Bunch (no-wake case)

Gaussian bunch

$f(v,\tau) = \frac{N_b}{2\pi\sigma u} e^{-v^2/2u^2 - \tau^2/2\sigma^2}$ — longitudinal distribution function,

$\rho(\tau) = \int_{-\infty}^{\infty} f(v,\tau)\,\mathrm{d}v = \frac{1}{\sqrt{2\pi}}\, e^{-\tau^2/2}$ — line density of a beam.

The head-tail mode equation for Gaussian bunch is

$$\boxed{\begin{cases} \bar{y}''(\tau) + \nu\, e^{-\tau^2/2}\, \bar{y}(\tau) = 0\,, \\ \bar{y}'(\pm\infty) = 0, \end{cases}}$$

where boundary conditions are selecting a sequence of eigenvalues, ν_k:

$$\nu_0 < \nu_1 < \ldots < \nu_k < \ldots \to \infty.$$

Corresponding to each eigenvalue there is a unique eigenfunction, $\bar{y}_k(\tau)$:

$$\int_{-\infty}^{\infty} \rho(\tau)\bar{y}_i(\tau)\bar{y}_j(\tau)\,\mathrm{d}\tau = \delta_{ij},$$

Eigenvalues, eigenweights and asymptotic values for the first 14 SSC modes of the Gaussian bunch.

k	**0**	**1**	**2**	**3**	**4**	**5**	**6**
ν_k	**0**	**1.34**	**4.32**	**8.9**	**15.05**	**22.79**	**32.1**
ω_k	**1**	**1.47**	**1.19**	**3.6**	**1.19**	**5.71**	**1.19**
$\lvert\bar{y}_k(\infty)\rvert$	**1**	**1.63**	**1.99**	**2.27**	**2.51**	**2.72**	**2.92**
k	**7**	**8**	**9**	**10**	**11**	**12**	**13**
ν_k	**42.98**	**55.44**	**69.47**	**85.08**	**102.26**	**121.01**	**141.34**
ω_k	**7.83**	**1.19**	**9.94**	**1.19**	**12.05**	**1.19**	**14.16**
$\lvert\bar{y}_k(\infty)\rvert$	**3.1**	**3.26**	**3.42**	**3.57**	**3.71**	**3.84**	**3.97**

First 16 eigenfunctions of the Gaussian bunch, $\bar{y}_k(\tau)$.

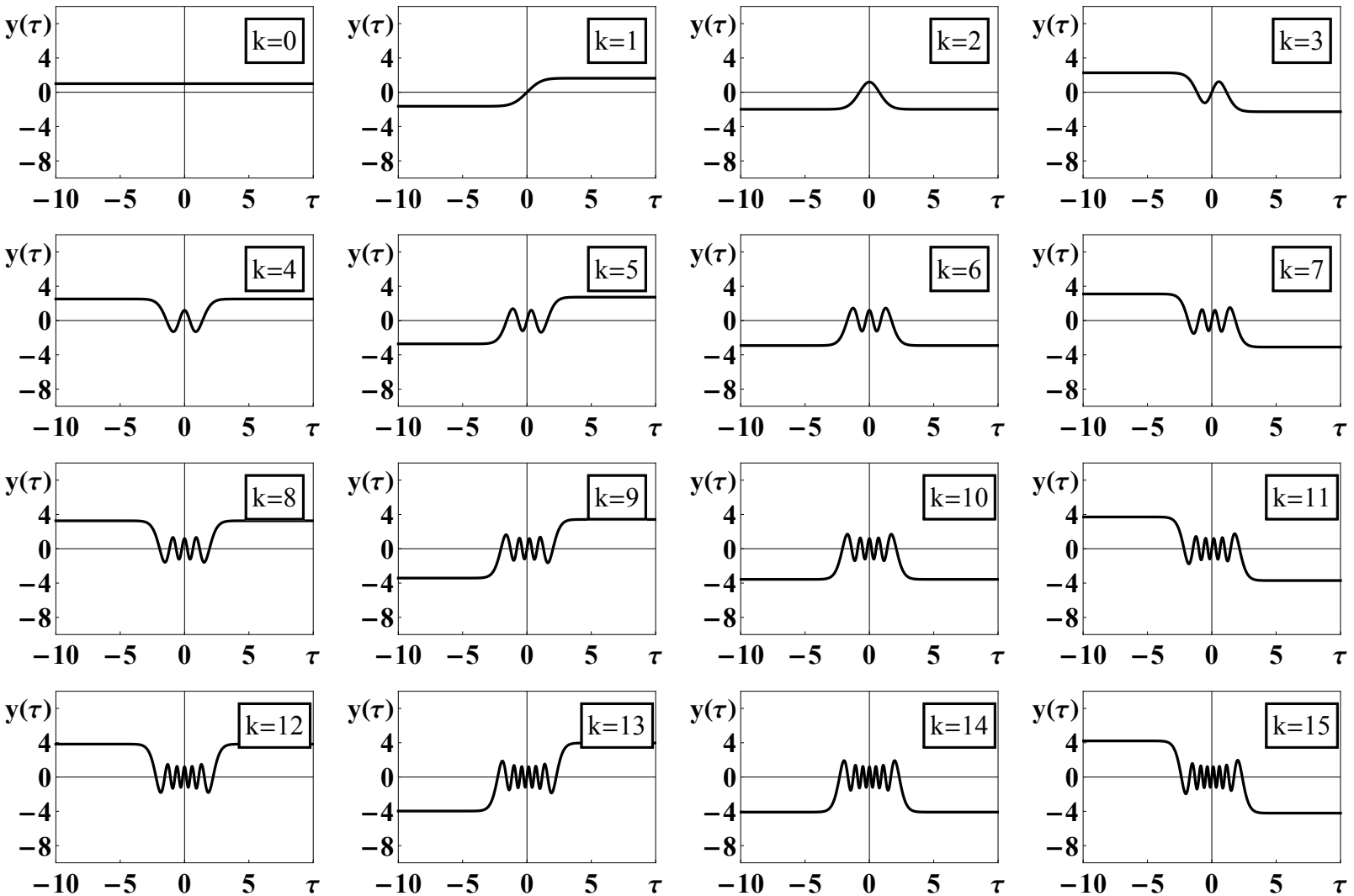

Modes don't depend on chromaticity, except head-tail phase $e^{-i\zeta\tau}$.

First 16 zero chromaticity local dipole moments, $\rho(\tau)\bar{y}_k(\tau)$.

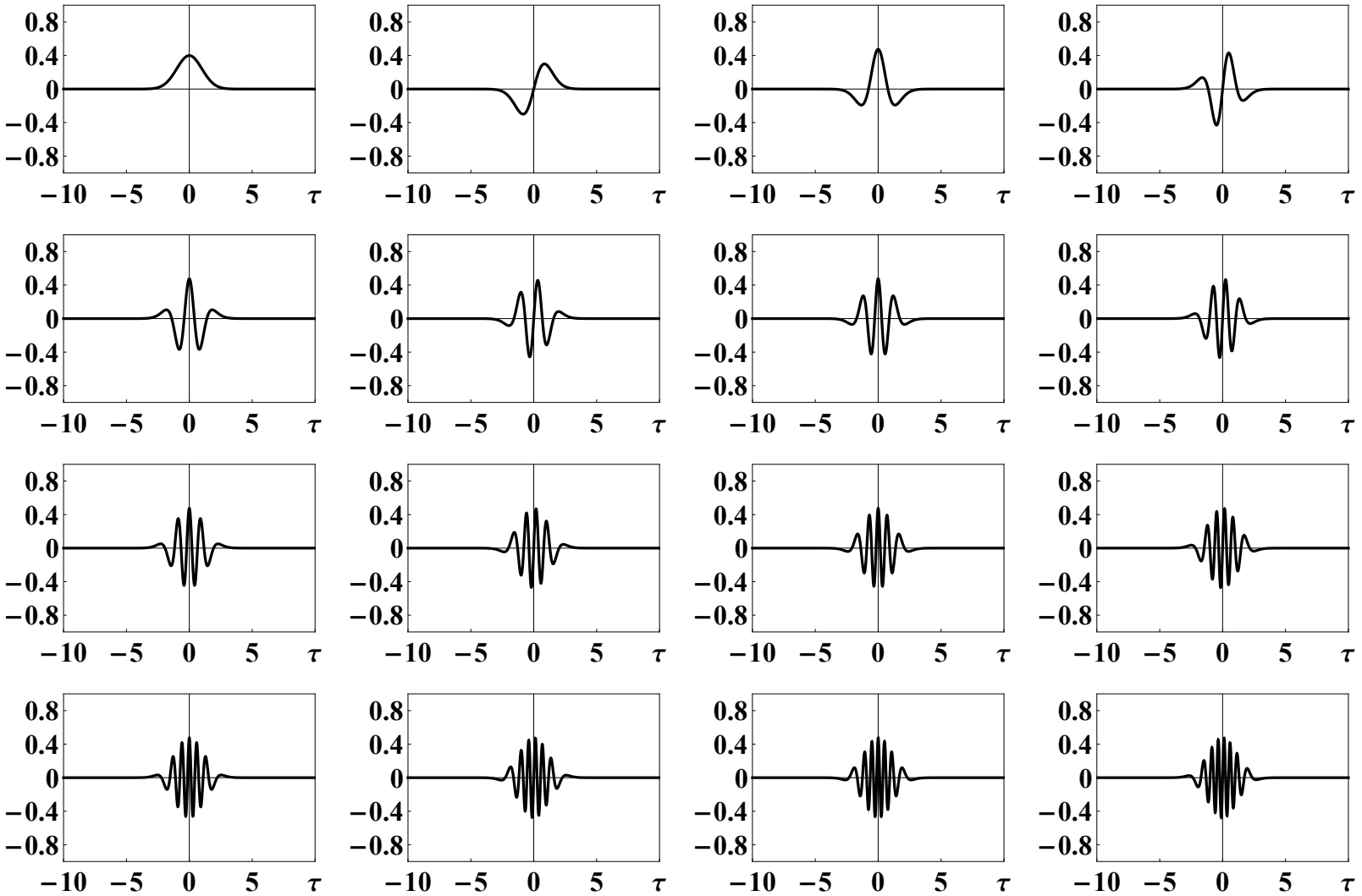

First 16 bunch dipole moments as a function of the head-tail phase, $I_k(\zeta) = \int_{-\infty}^{\infty} \rho(\tau)\bar{y}_k(\tau)e^{i\zeta\tau}\,\mathrm{d}\tau$.

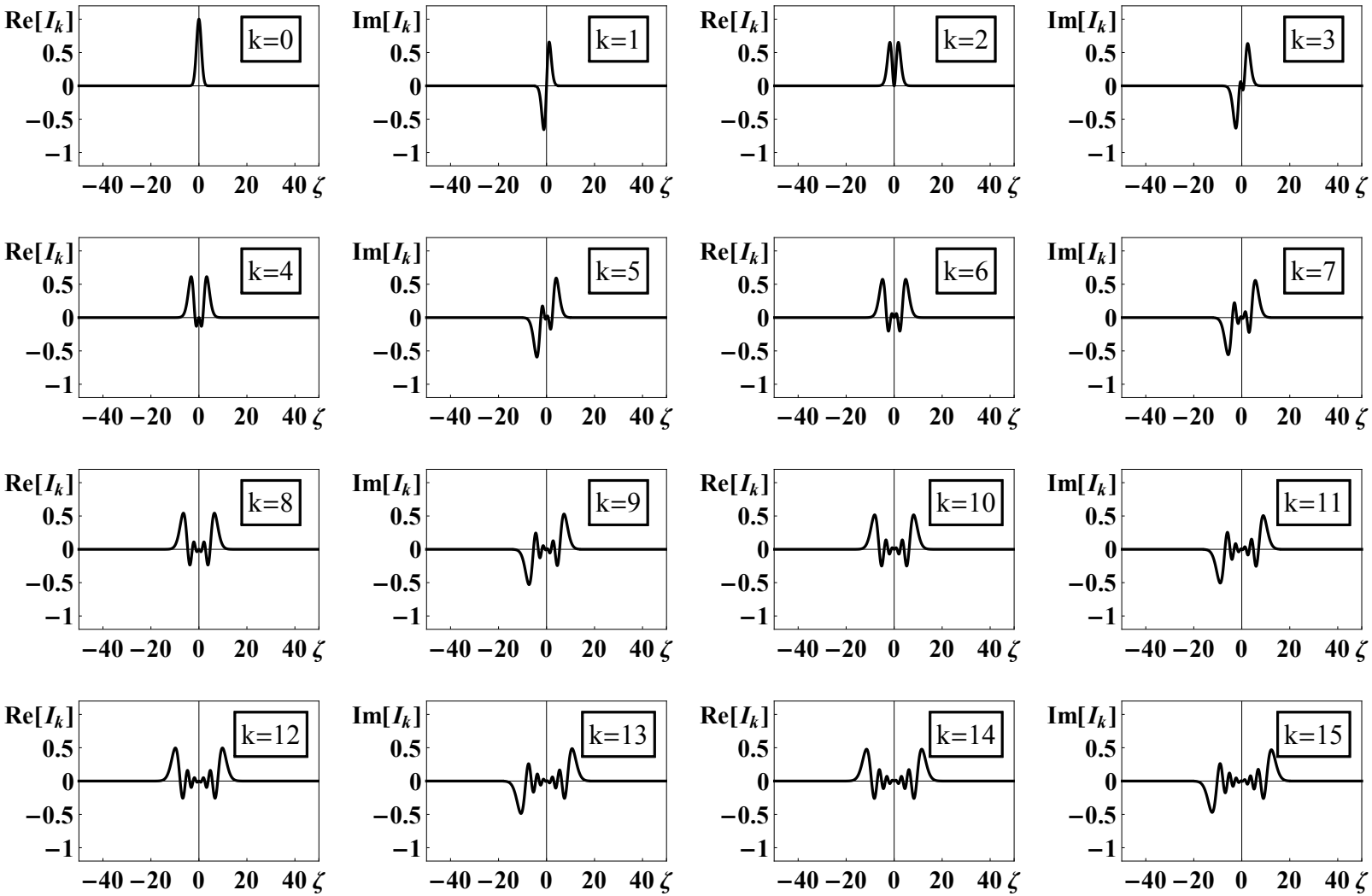

2.2 Wake Forces, $Q_w \gg Q_s^2/Q_{\max}$

$$\bar{y}(\tau)'' + \nu\, e^{-\tau^2/2}\, \bar{y}(\tau) = \varkappa \left(\hat{\mathrm{W}} + \hat{\mathrm{D}}\right) \bar{y}(\tau).$$

Driving and detuning wakes, $\hat{\mathrm{W}}$ and $\hat{\mathrm{D}}$.

$$\begin{aligned} \hat{\mathrm{W}}\, \bar{y}(\tau) &= \int_{\tau}^{\infty} W(\tau-\sigma)\rho(\sigma)\bar{y}(\sigma) e^{i\zeta(\tau-\sigma)}\, \mathrm{d}\sigma, \\ \hat{\mathrm{D}}\, \bar{y}(\tau) &= \bar{y}(\tau) \int_{\tau}^{\infty} D(\tau-\sigma)\rho(\sigma)\, \mathrm{d}\sigma, \end{aligned}$$

with corresponding matrix elements in no-wake modes basis

$$\begin{aligned} \hat{\mathrm{W}}_{lm} &= \int_{-\infty}^{\infty}\int_{\tau}^{\infty} W(\tau-\sigma)\rho(\tau)\rho(\sigma)\bar{y}_l(\tau)\bar{y}_m(\sigma) e^{i\zeta(\tau-\sigma)}\, \mathrm{d}\sigma\, \mathrm{d}\tau, \\ \hat{\mathrm{D}}_{lm} &= \int_{-\infty}^{\infty}\int_{\tau}^{\infty} D(\tau-\sigma)\rho(\tau)\rho(\sigma)\bar{y}_l(\tau)\bar{y}_m(\tau)\, \mathrm{d}\sigma\, \mathrm{d}\tau. \end{aligned}$$

Resistive wall impedance

Wake function over a distance L:

$$W_m(z<0) = \frac{2\,J_{\rm vc}}{\pi\, b^{2m+1}(1+\delta_{m0})}\sqrt{\frac{c}{\sigma_s}}\frac{L}{\sqrt{|z|}}.$$

- b — vacuum chamber radius
- $J_{\rm vc}$ — Yokoya factor, is equal to 1 for round vacuum chamber, and, $\frac{\pi^2}{24}$ and $\frac{\pi^2}{12}$ for horizontal and vertical directions for a flat chamber.

Below we will provide the results for $W_1(\tau)$ and for convenience we will factor out all numerical coefficients:

$$\tilde{\varkappa} = \frac{Q_{\rm eff}(0)}{Q_s^2}\frac{r_0 R}{4\pi\beta^2\gamma Q_b}\frac{2\,L\,J_{\rm vc}\sqrt{c/\sigma_s}}{\pi\, b^3}.$$

2.2.1 Driving wake

$$\hat{\mathrm{W}}_{lm} = (-1)^m \left[\frac{1-i}{\sqrt{2}} \int_{-\infty}^{\zeta} \frac{I_l(\omega) I_m(\omega)}{\sqrt{\zeta - \omega}} \frac{\mathrm{d}\omega}{2\sqrt{\pi}} + \frac{1+i}{\sqrt{2}} \int_{\zeta}^{\infty} \frac{I_l(\omega) I_m(\omega)}{\sqrt{\omega - \zeta}} \frac{\mathrm{d}\omega}{2\sqrt{\pi}} \right]$$

Absolute value of 10 by 10 driving resistive wall wake matrices, $\hat{W}_{lm}$, plotted for different values of head-tail phase ($\zeta = 0, 2, 4, 8$).

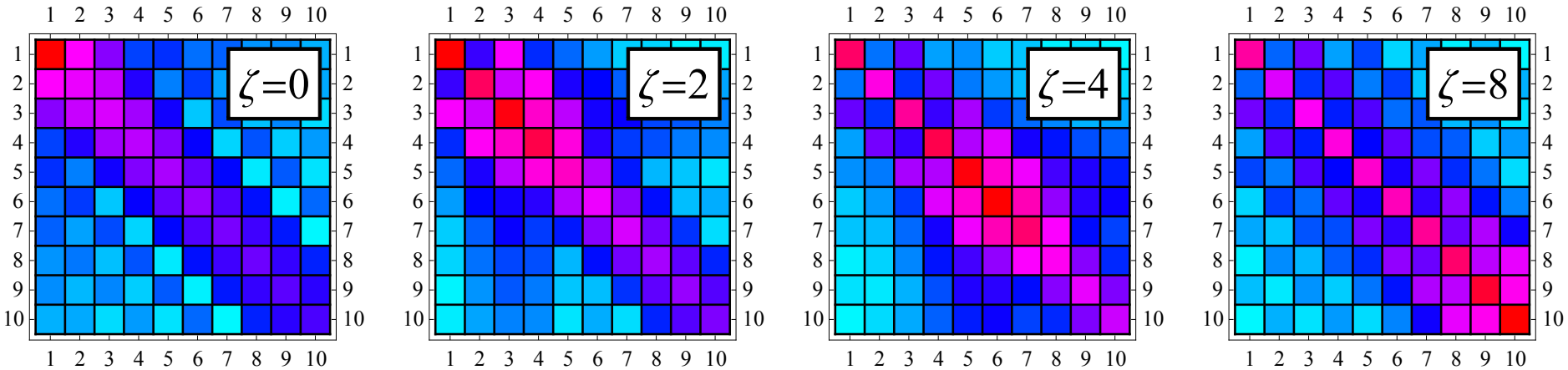

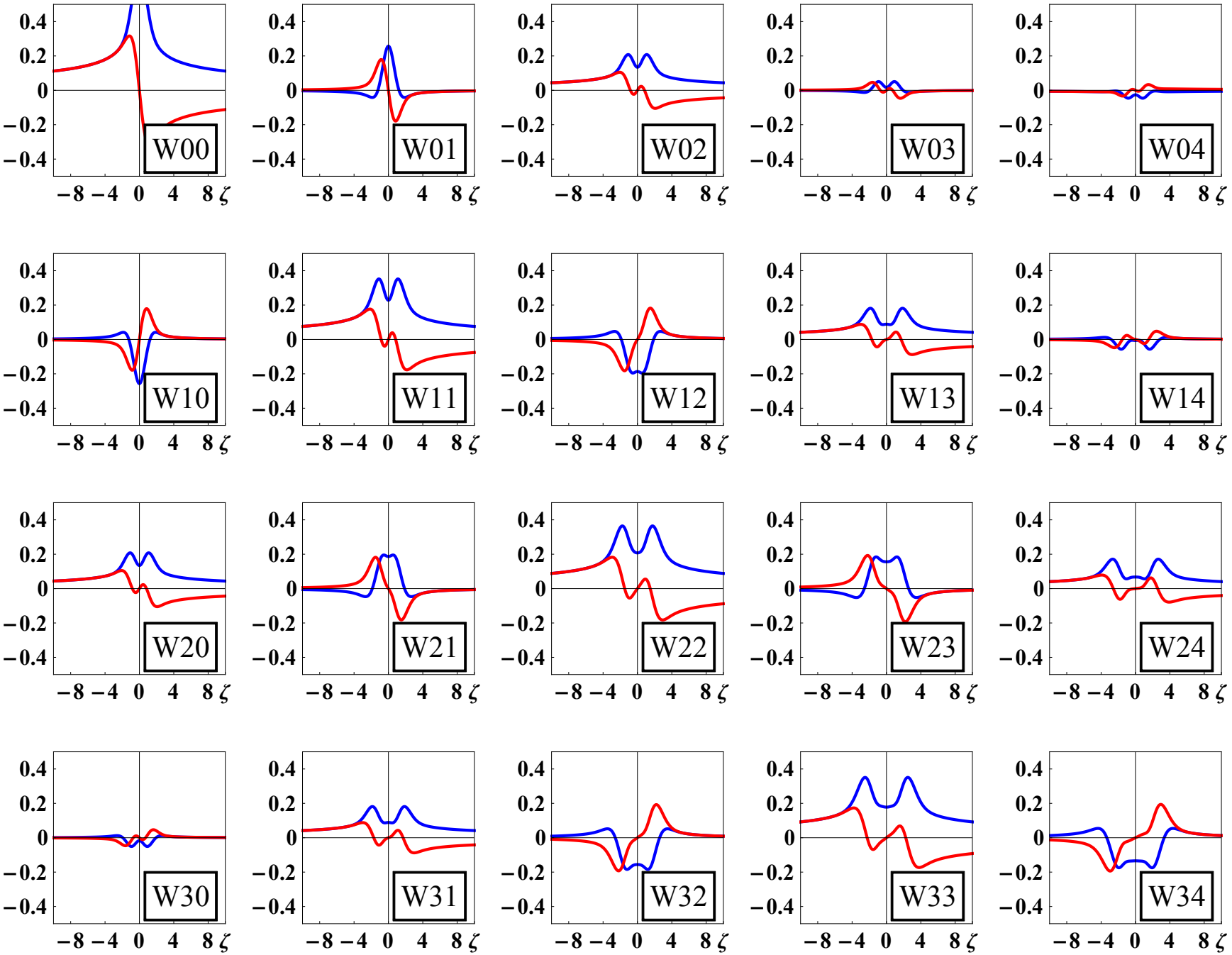
W00
W01
W02
W03
W04
W10
W11
W12
W13
W14
W20
W21
W22
W23
W24
W30
W31
W32
W33
W34
0.4
0.2
0
−0.2
−0.4
−8 −4 0 4 8 ζ

2.2.2 Detuning wake

$$\hat{\mathrm{D}}_{lm} = \int_{-\infty}^{\infty} \mathbf{D}(\tau)\rho(\tau)\bar{y}_l(\tau)\bar{y}_m(\tau)\,\mathrm{d}\tau \quad \text{where} \quad \mathbf{D}(\tau) = \int_0^{\infty} \frac{\rho(\sigma+\tau)}{\sqrt{\sigma}}\,\mathrm{d}\sigma.$$

Wake quadrupole field along the bunch for resistive wall impedance, $\mathbf{D}(\tau)$, and values of 40x40 detuning resistive wall wake matrix, $\hat{D}_{lm}$.

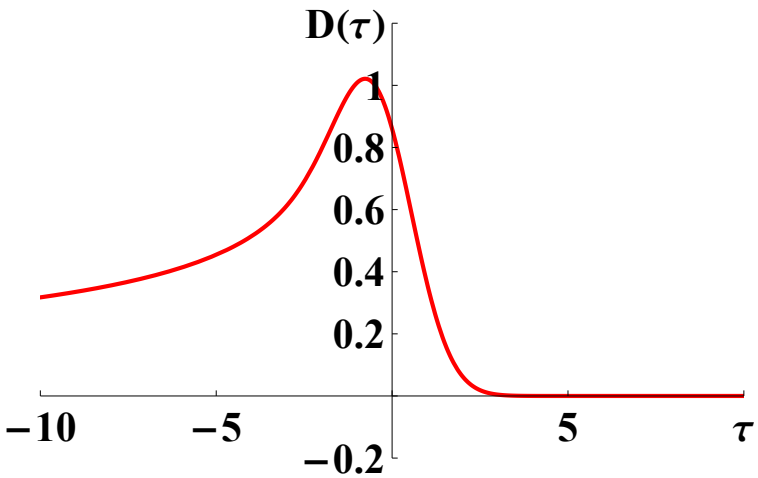

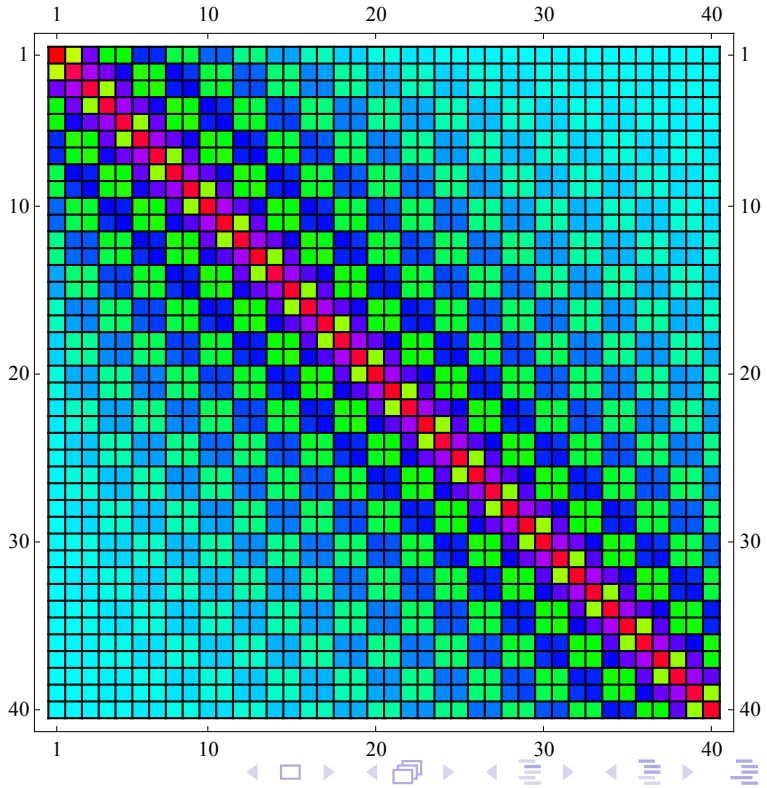

2.3 Damper and Dipole Moments Direct Product Matrix

$\bar{y}''(\tau) + \nu\, e^{-\tau^2/2}\, \bar{y}(\tau) = g\, \hat{G}\bar{y}(\tau)$, where g is a dimensionless gain.

Dipole moments direct product matrix

$$\hat{G}_{lm}(\zeta) = \int_{-\infty}^{\infty}\int_{-\infty}^{\infty} \rho(\tau)\rho(\sigma)\bar{y}_l(\tau)\bar{y}_m(\sigma)e^{i\zeta(\tau-\sigma)}\,\mathrm{d}\sigma\,\mathrm{d}\tau = (-1)^m I_l(\zeta)I_m(\zeta)$$

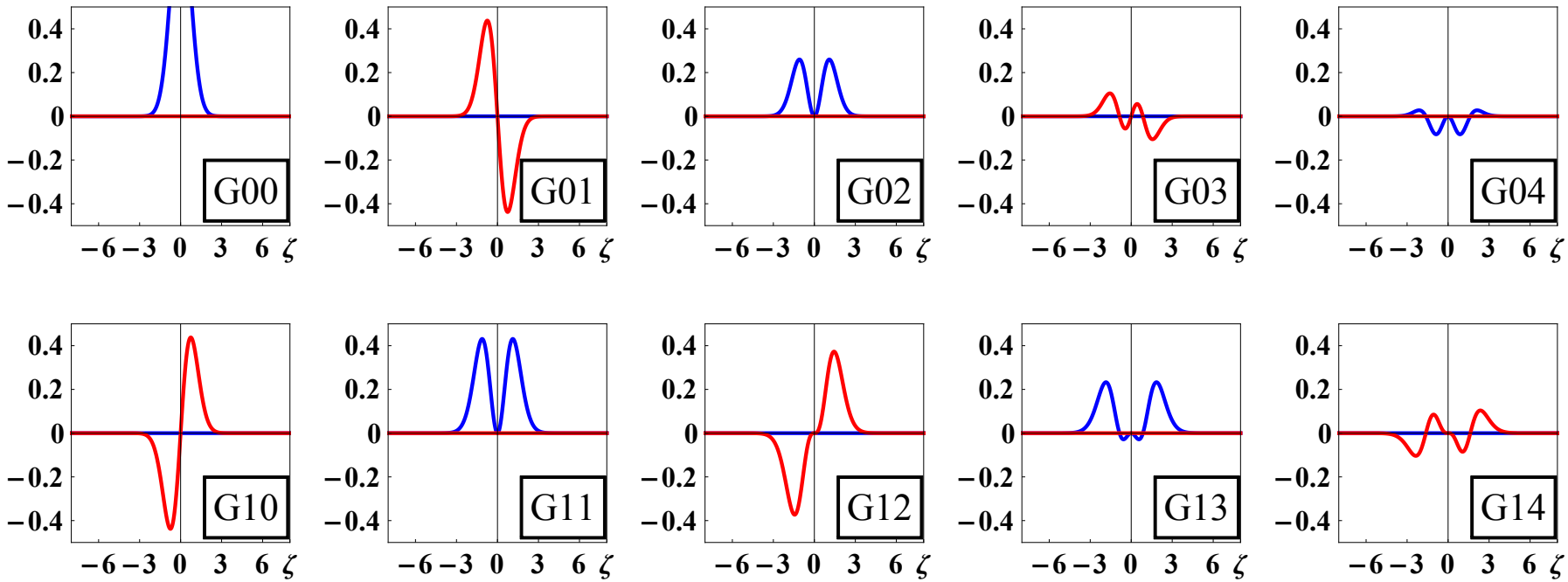

Absolute value of 40x40 dipole moments direct product matrices, $\hat{G}_{lm}$, for different values of head-tail phase ($\zeta = 0, 2, 4, 8, 16, 32$).

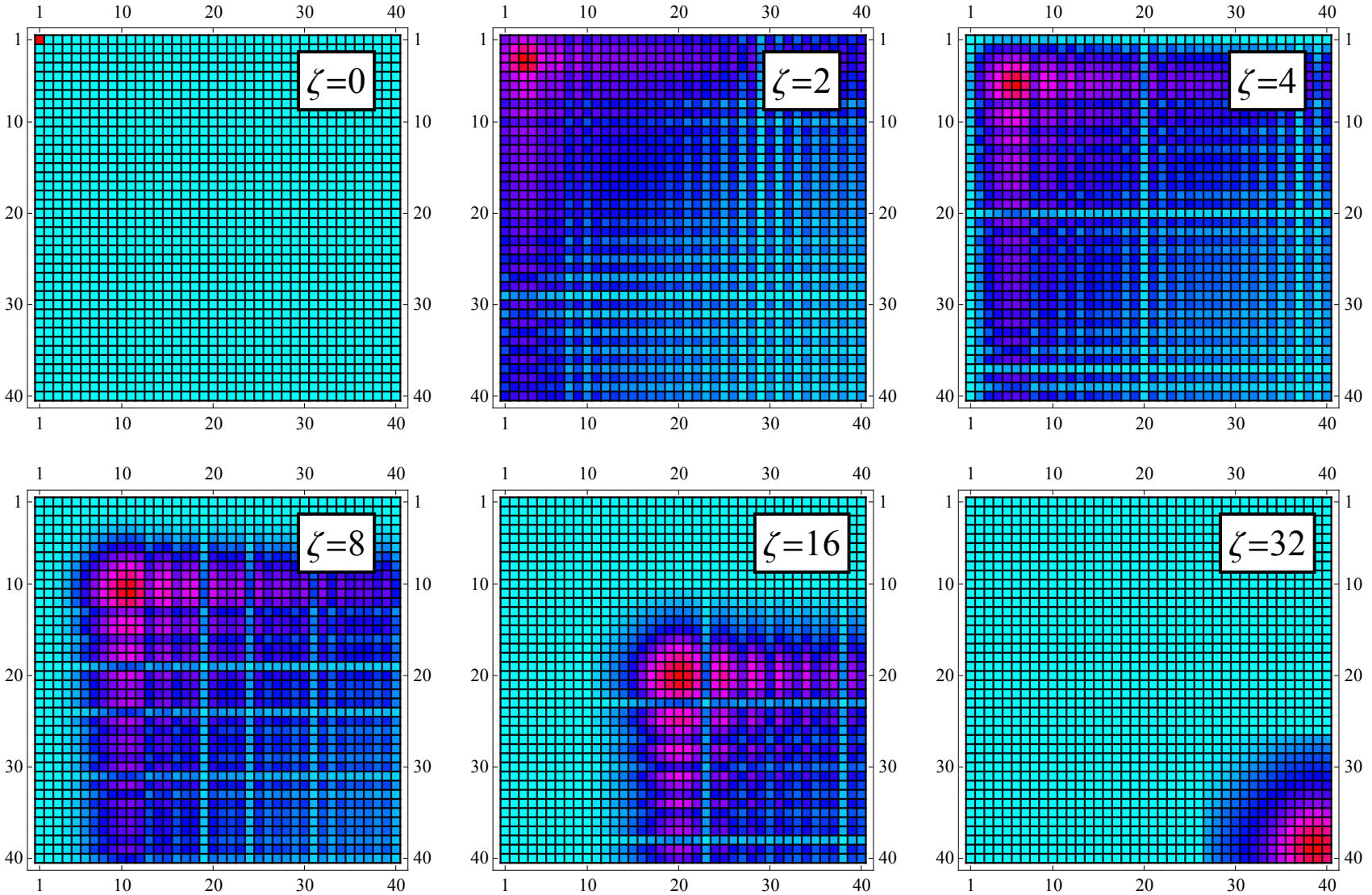

2.4 Stability Analysis

$$y(\tau)'' + \nu\, e^{-\tau^2/2}\, y(\tau) = \varkappa \left(\hat{\mathrm{W}} + \hat{\mathrm{D}}\right) y(\tau) + g\, \hat{\mathrm{G}}\, y(\tau).$$

Solution expanded over the no-wake basis, $\tilde{y}(\tau) = \sum_{k=0}^{\infty} C_k \bar{y}_k(\tau)$.

Linear matrix problem for eigensystem:

$$\left[\varkappa \left(\hat{\mathrm{W}} + \hat{\mathrm{D}}\right) + g\, \hat{\mathrm{G}} + \mathrm{diag}\{\nu\}\right] \mathbf{C} = \tilde{\nu}\mathbf{C},$$

where $\mathbf{C} = [C_0, C_1, C_2, \ldots]^{\mathrm{T}}$ is a vector of coefficients C_i to be determined from eigensystem problem, and, $\mathrm{diag}\{\nu\}_{lm} = \nu_l \delta_{lm}$ is a diagonal matrix whose k-th diagonal element is a k-th eigenvalue of the no-wake case.

First ten coherent tunes of the Gaussian bunch for zero chromaticity and resistive wake as functions of wake amplitude, $\tilde{\varkappa}$.

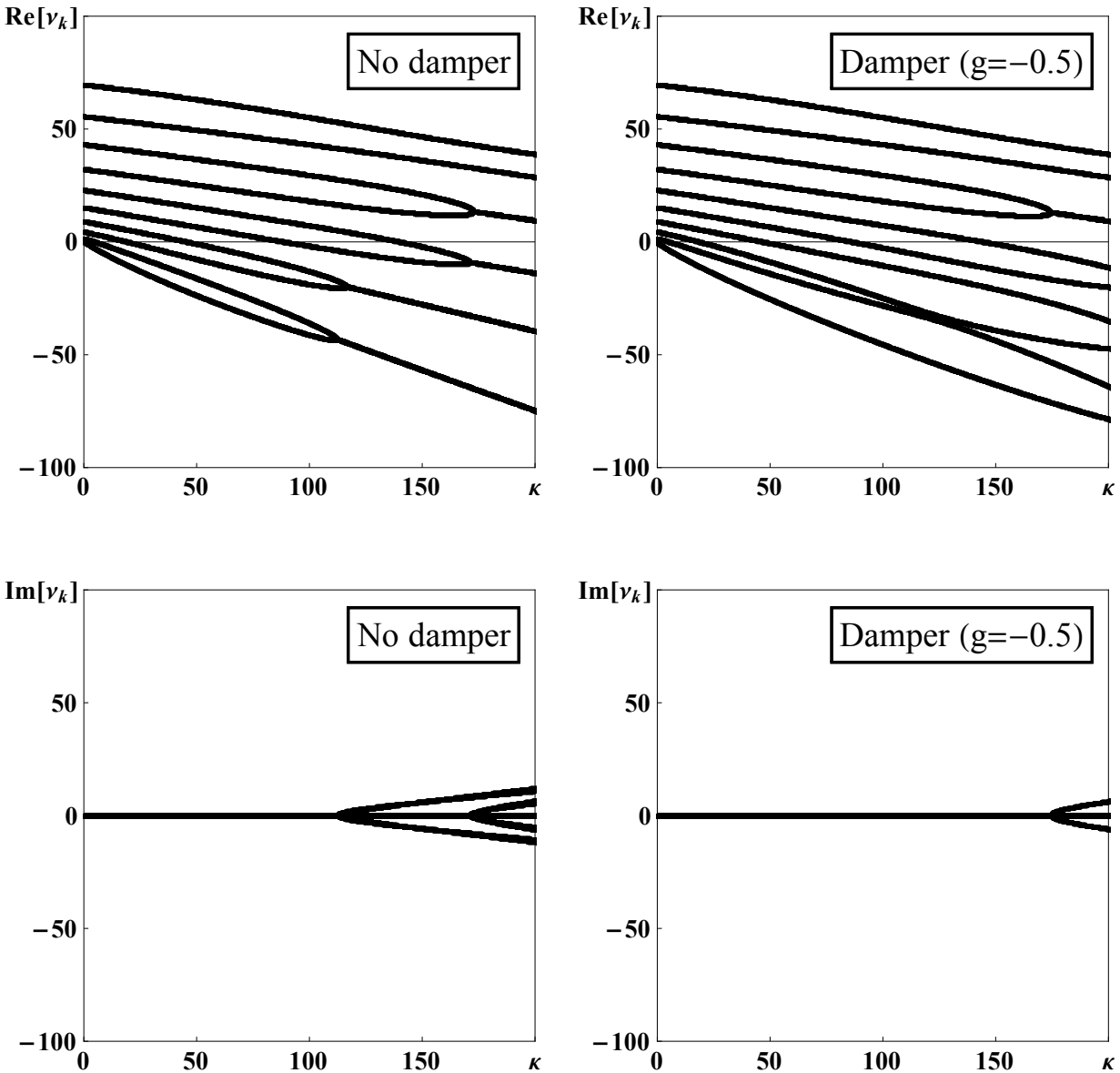

3. Head-Tail Modes in Booster

Motivation

- The SSC theory should be compared with both, simulations and experiment.
- Usually only particular head-tail mode can be observed in experiment when the beam is in unstable regime. We tried new approach performing observation from stable machine operation exciting modes by pinging a beam every 500 turns.

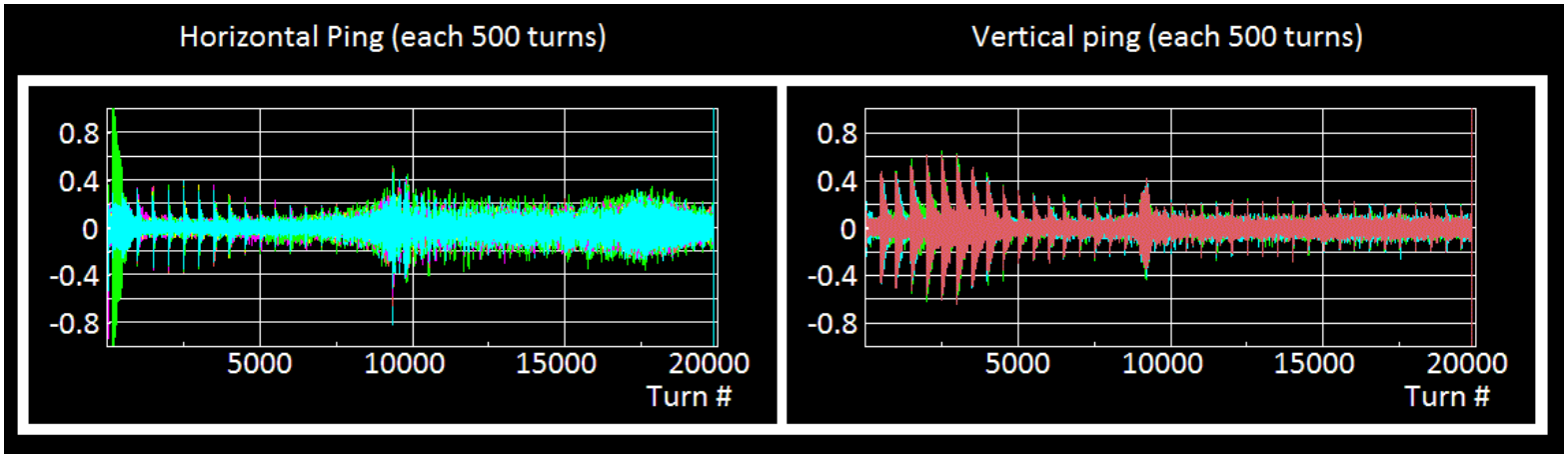

3.1 Experimental Setup

Measuring circuit

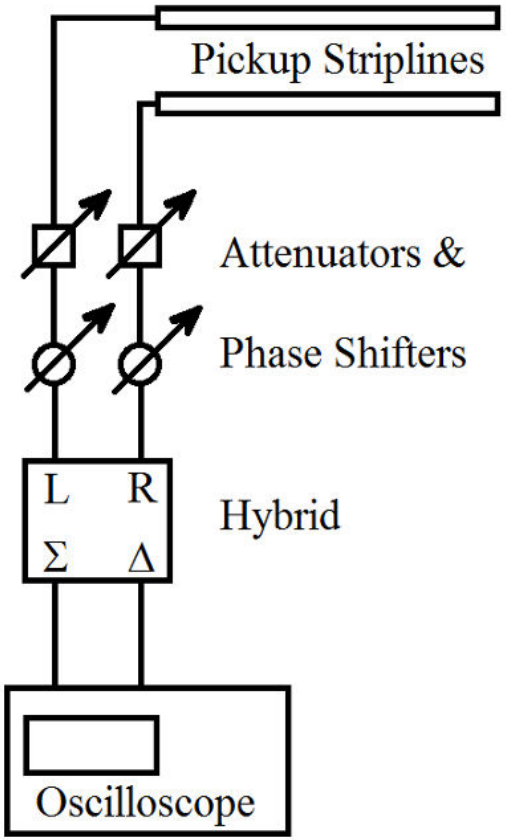

Impedance in a time domain

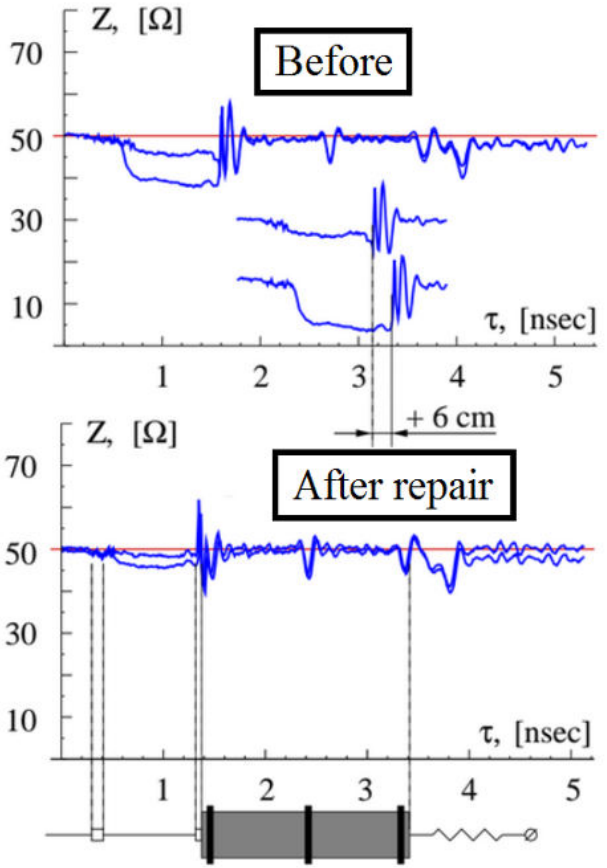

Experiment parameters

The experimental data gathered for the regular operational setup of the Booster. Three different intensities provided by 3, 7 and 14 turns of injection from LINAC have been studied; corresponding values of number of particles injected into the machine are 0.63, 2.01 and 4.26×10^{12}.

One can note the distinguishing lost of particles due to collective instability at the transition for highest intensity.

Beam intensities for Booster cycle.

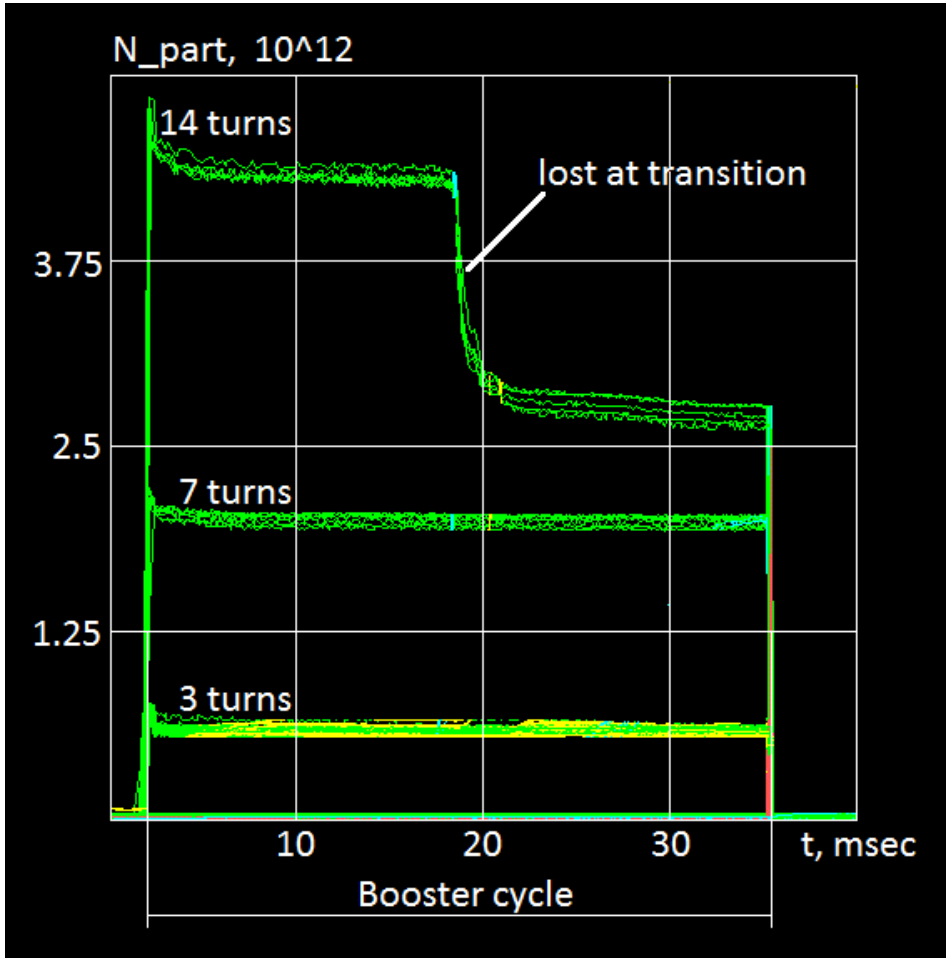

3.2 Decomposition of head-tail modes

In order to extract head-tail modes, one can construct the following matrix consisting of difference signals obtained for different bunches and N turns

$$\left[\Delta^{(1)}(1), \Delta^{(1)}(2), \ldots, \Delta^{(1)}(N), \ldots, \Delta^{(84)}(1), \Delta^{(84)}(2), \ldots, \Delta^{(84)}(N)\right]^{\mathsf{T}}$$

Performing the singular value decomposition (SVD) one will obtain spatial and time modes along with corresponding singular values showing the amplitudes; $\Delta(\tau)/\sqrt{\rho(\tau)}$ should be used to satisfy normalization of $\bar{y}_k(\tau)$.

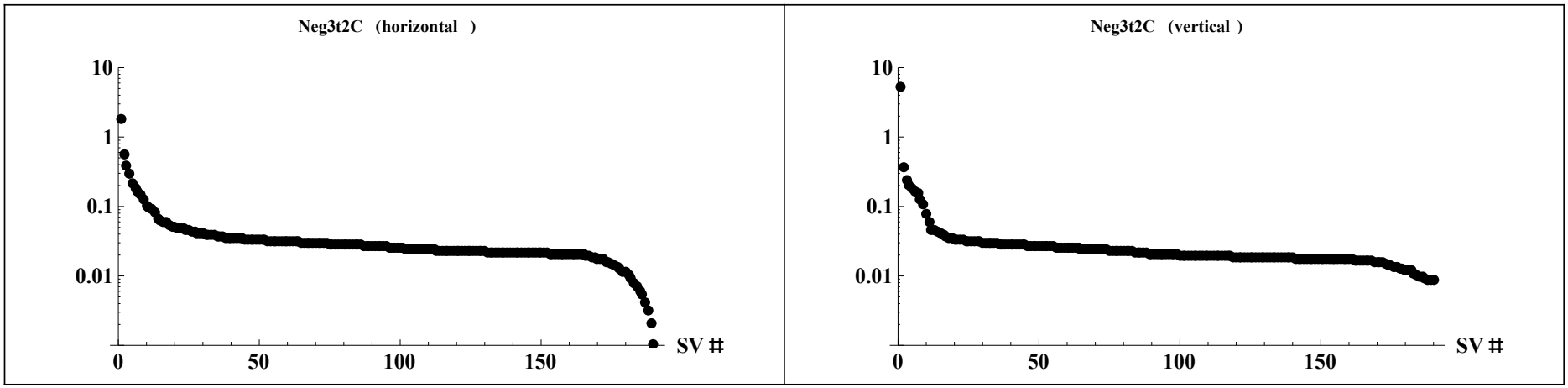

3.2.1 Modes right before transition (16.40 msec)

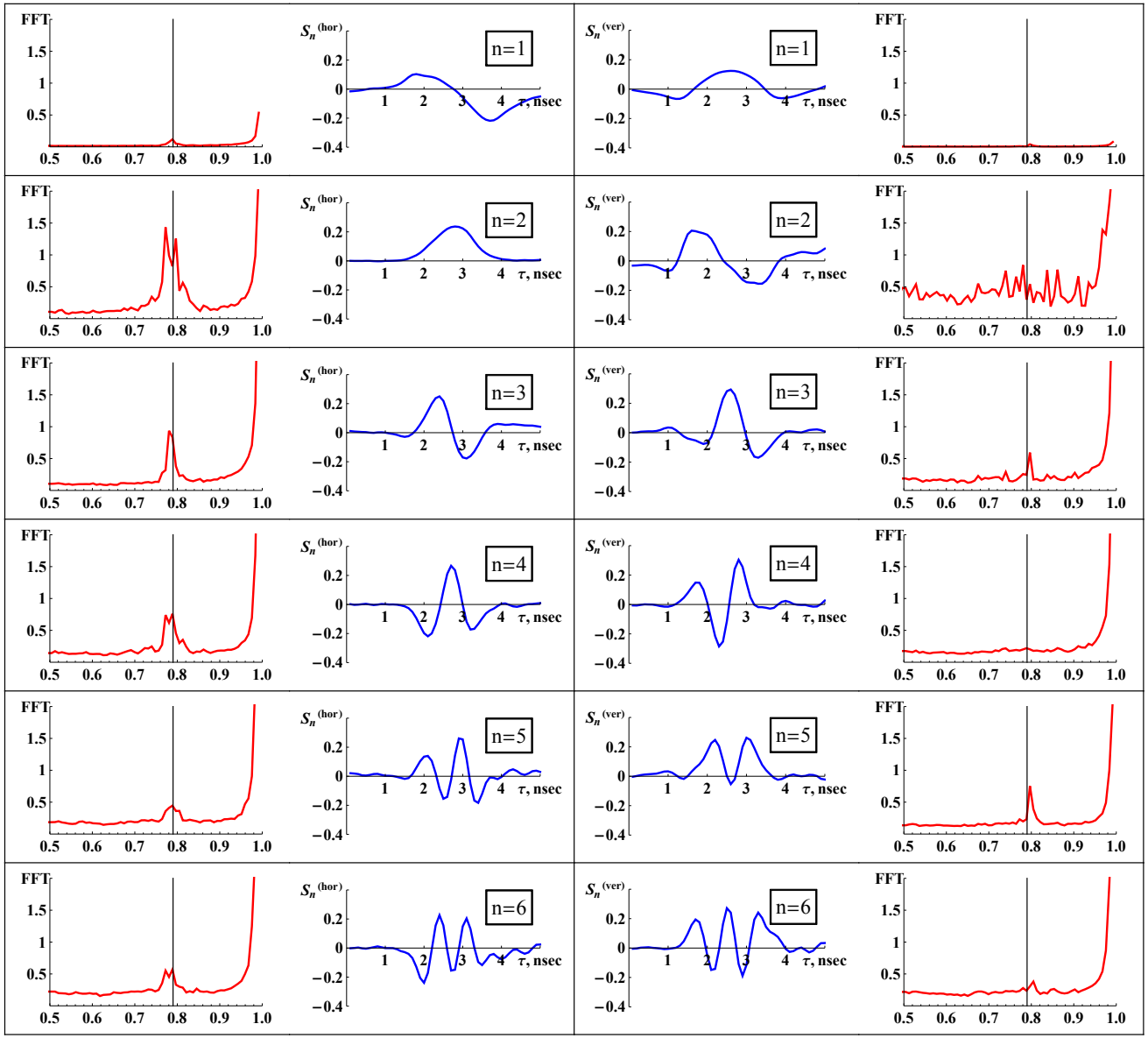

First 16 zero chromaticity local dipole moments, $\rho(\tau)\bar{y}_k(\tau)$.

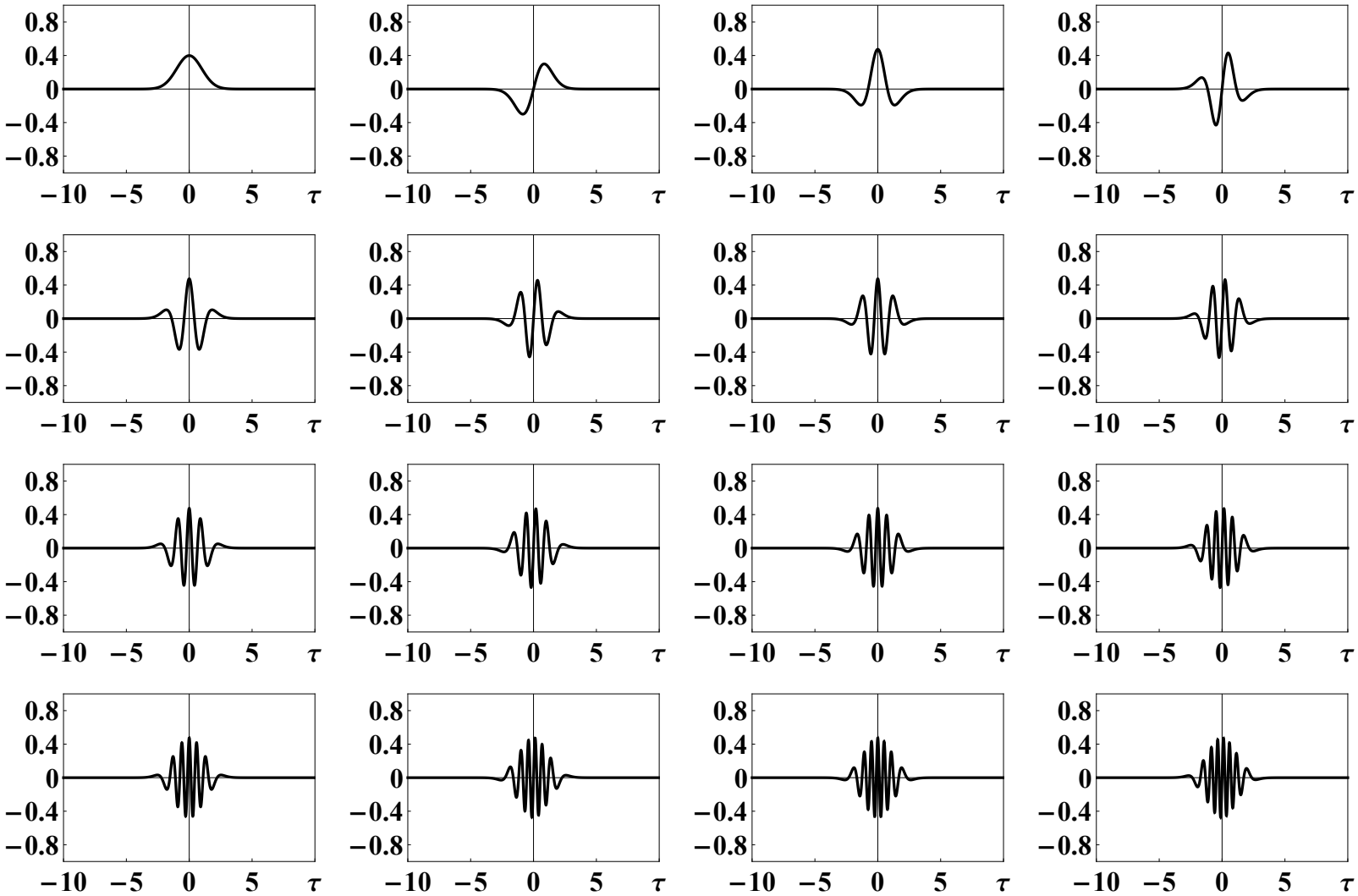

7 turns

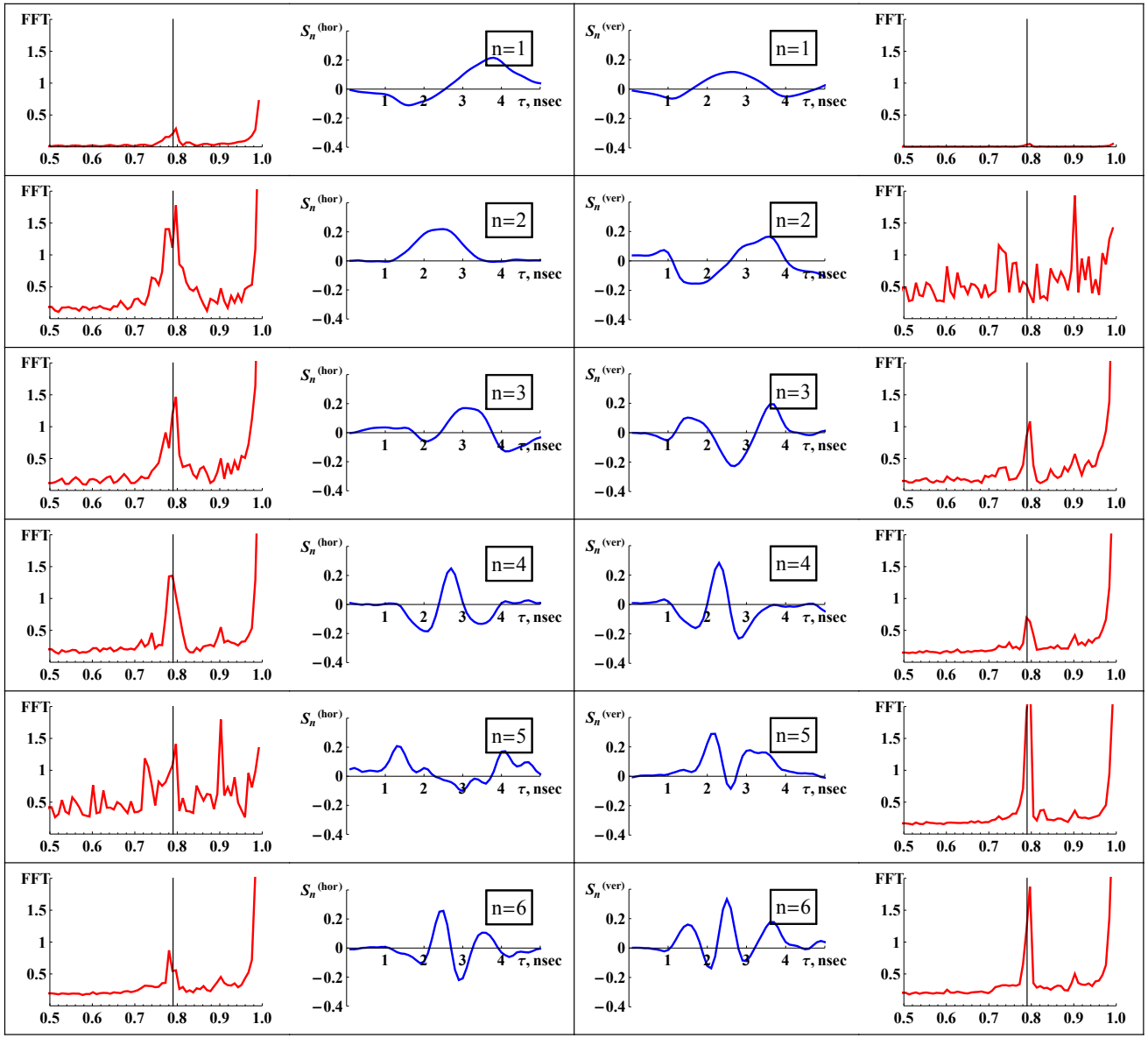

14 turns

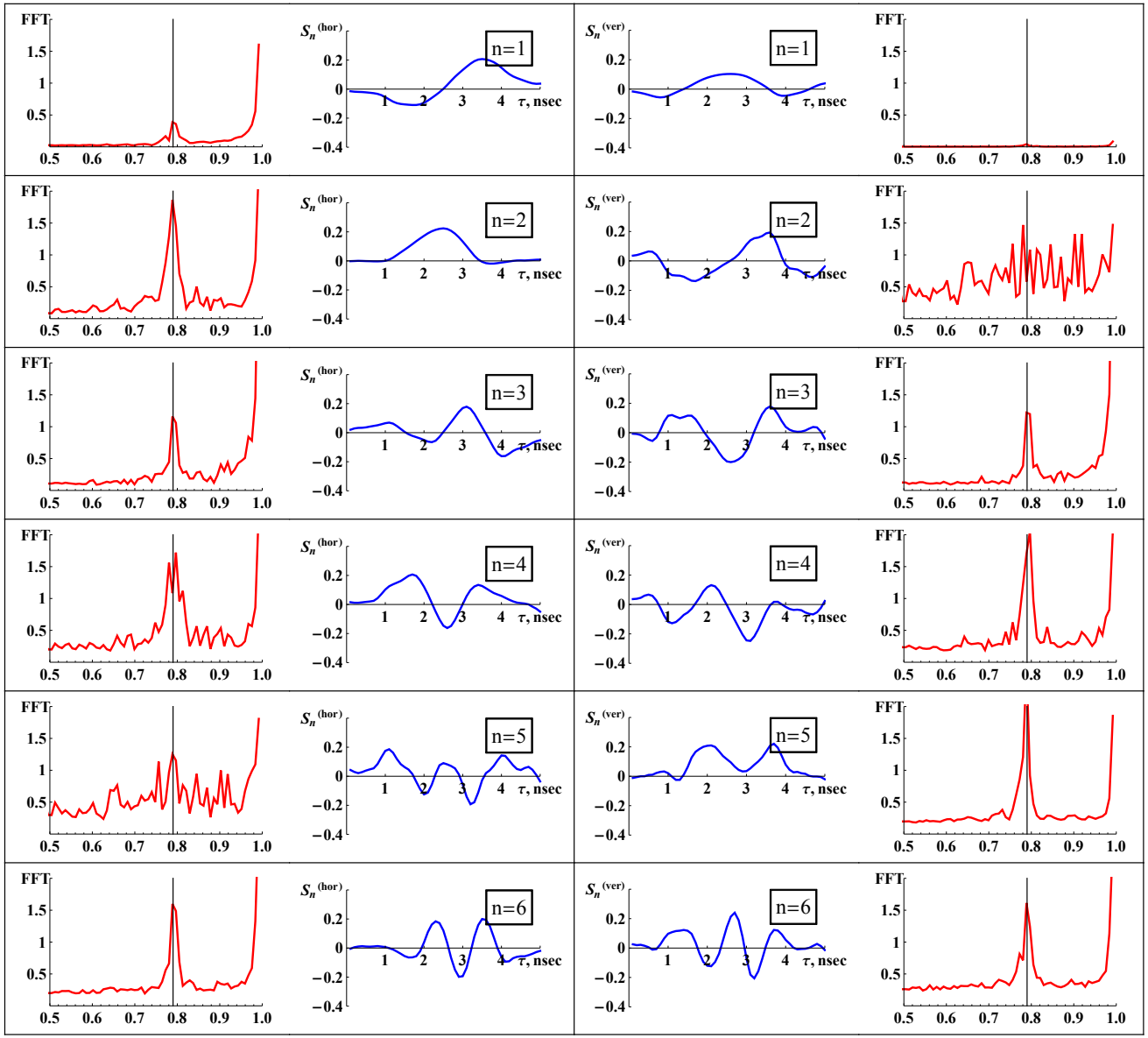

3.2.2 Modes at the beginning of the cycle (2.84 msec)

Consider a case when the signal from the BPM strip line is overlapped

$$V(t) \propto \exp\left[\frac{-(t+\tau)^2}{2\sigma^2}\right] - \exp\left[\frac{-(t-\tau)^2}{2\sigma^2}\right], \qquad \tau < \sigma.$$

The signal decomposition can be performed using recurrent shift
$V(t,\tau) + V(t-2\tau,\tau) = V(t,2\tau)$

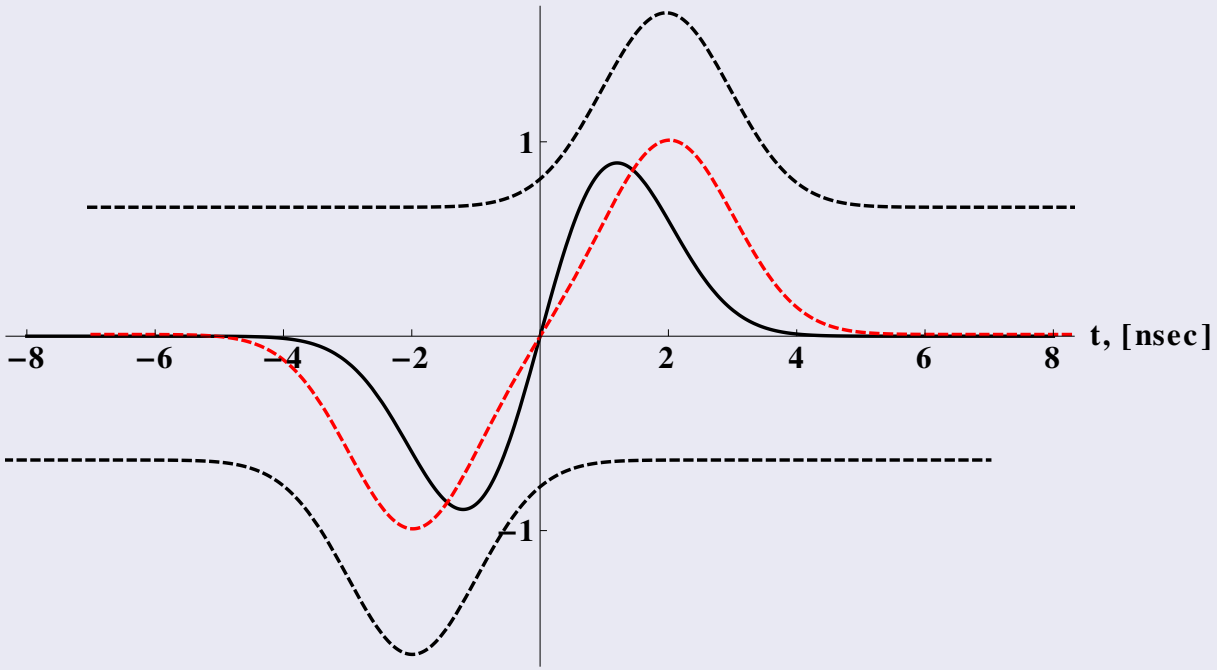

3 turns

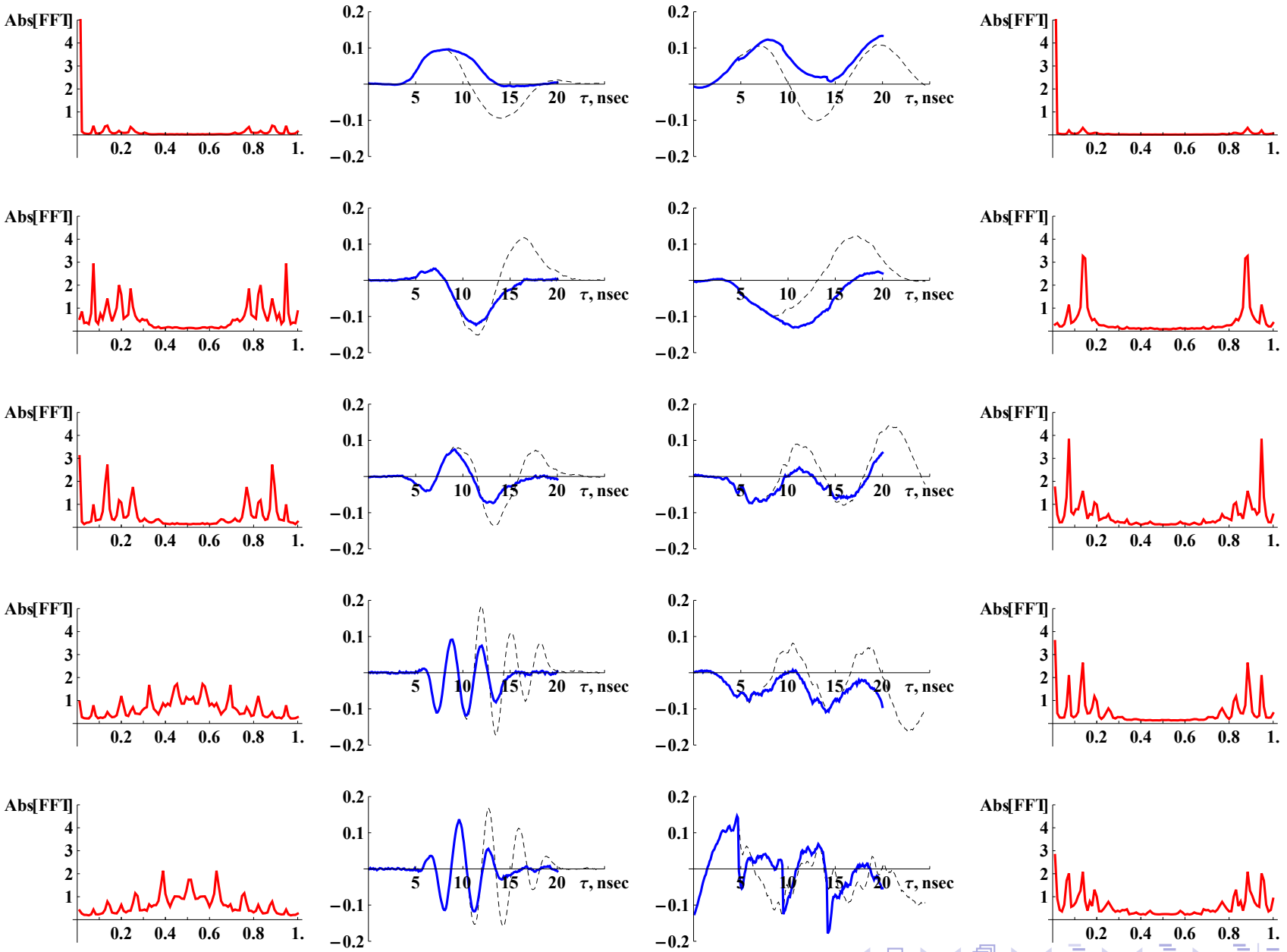

7 turns

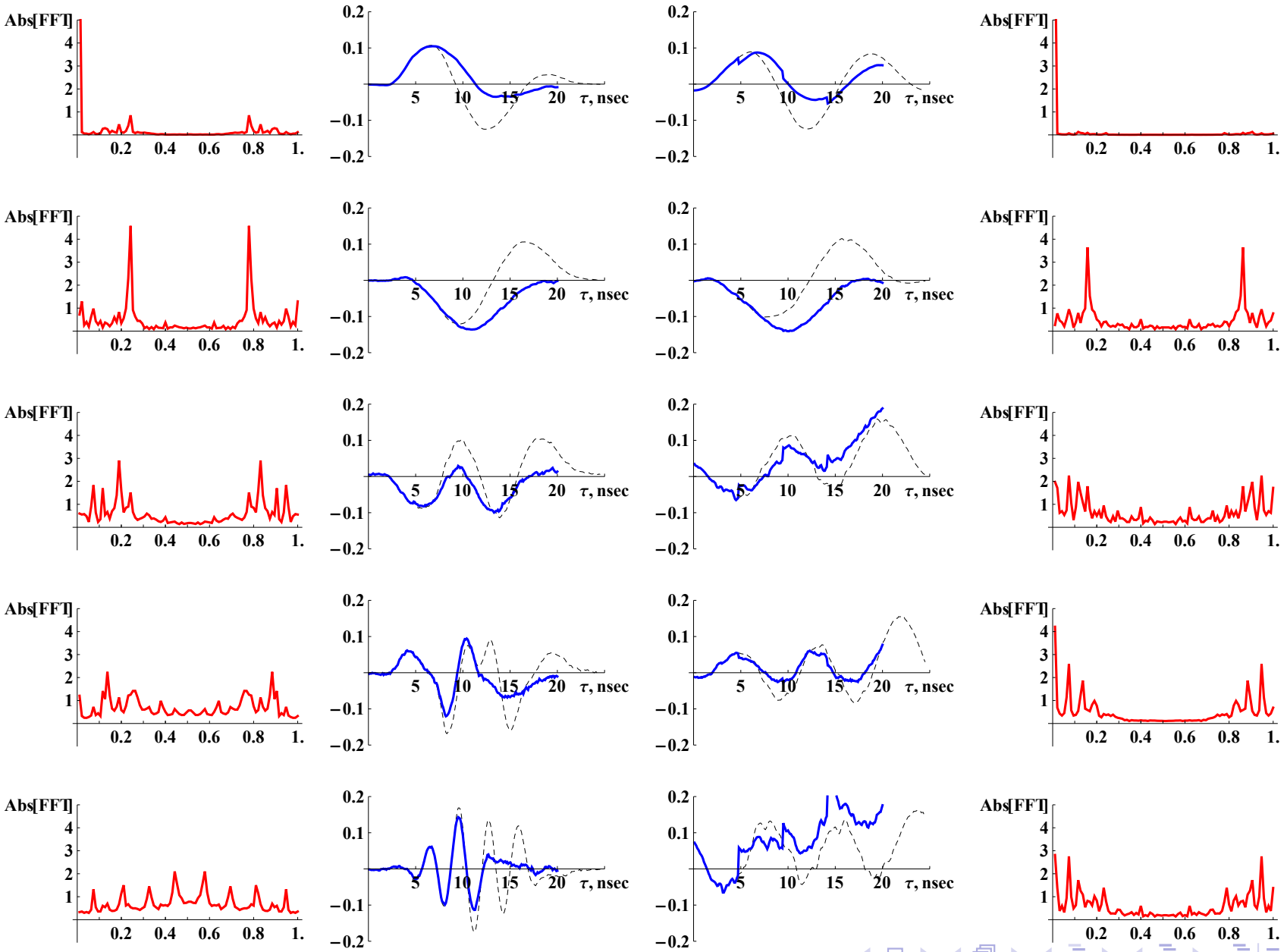

14 turns

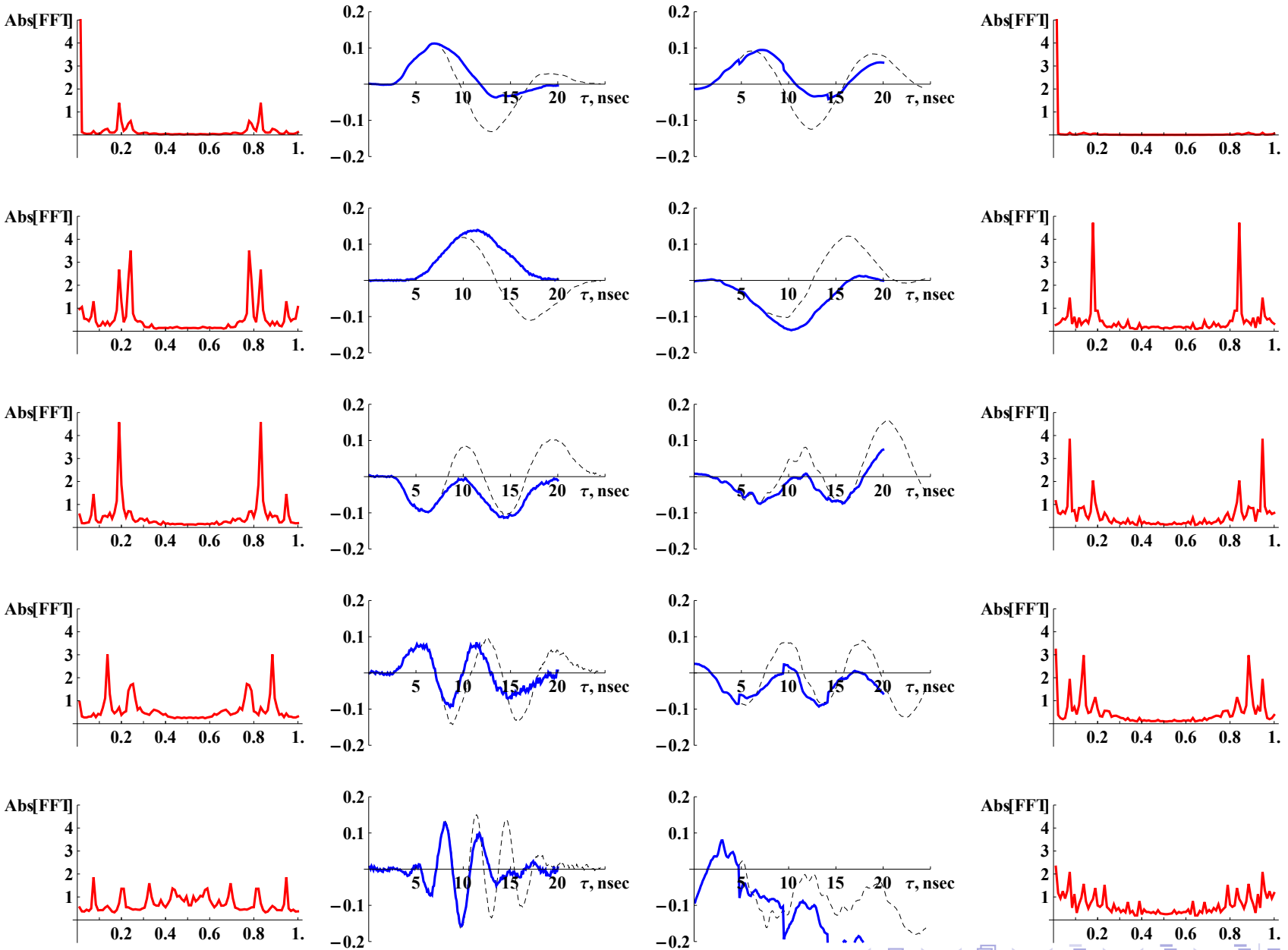

4.2 SSC theory

- A more precise analysis of a general equation for the modes for the Gaussian bunch and numerical calculations of the spatial shapes of modes as well as their eigenfrequencies for the no wake case.
- Numerical calculation of the matrices of the driving and detuning wake operators for the resistive wakes, $\hat{W}_{lm}$ and $\hat{D}_{lm}$ respectively.
- Inclusion of a linear bunch-by-bunch damper and coupled bunch interaction into the theory through the dipole moments direct product matrix, $\hat{G}_{lm}$ matrix. It should be noticed that not bunch-by-bunch effects can be easily included into the model by the use of derivatives of $\hat{D}_{lm}$ with respect to head-tail phase parameter, .
- Further use of created numerical tool will help to understand the collective stability for space charge dominated beams depending on damper parameters. It can be directly applied for both FermiLab Booster and Recycler rings after inclusion of proper wake matrices.

4.3 Head-tail modes experiment

- Directly observation of head-tail modes from the stable beam motion in FermiLab Booster ring has been performed (up to 10 modes for both horizontal and vertical degrees of freedom associated with collective beam motion can be extracted).
- Spatial shape of modes are very close to the prediction of SSC theory. The qualitative agreement in between theory and experiment has been demonstrated.
- Notwithstanding that experimental setup were pushed to the available limit, unfortunately the resolution of collected data did not allow to resolve eigenfrequencies.
- The change of modes' shape is in agreement with theory prediction: the increase in intensity enhance the wake forces influence and modes becomes more asymmetric.

Acknowledgment

I want to acknowledge

- My supervisor Prof. **Young-Kee Kim**
- **Valeri Lebedev** and **Alexey Burov** for useful discussions and multiple suggestions on data analysis
- **Sergey Nagaitsev**, **Slava Danilov**, **Yaroslav Kharkov** and espesially **Ivan Morozov** for participating in studies of non-linear dynamics and integrable optics
- **Kent Triplett** for his great assistance in the control room during all experiments
- **Brian Fellenz** and **Nathan Eddy** for their help with experimental settings
- All FermiLab control room people

“THANK YOU”.

Questions ?

Appendix A. Booster ring and beam parameters

Transverse motion parameters		
Max horizontal beta function, $\beta_{x,\,\mathrm{max}}$	(m)	33.7
Max vertical beta function, $\beta_{y,\,\mathrm{max}}$	(m)	20.5
Betatron tune, $\nu_{x,y}$		6.7
Phase advance per cell, $\mu_{x,y}$	($^\circ$)	96
Maximum dispersion	(m)	3.2
Longitudinal motion parameters		
Harmonic number, h		84
Injection RF frequency, f_{RF}	(MHz)	37.77
Extraction RF frequency, f_{RF}	(MHz)	52.81
Maximum RF voltage	(MV)	0.86

Booster structure		
Cell type		FOFDOOD
# of bend magnets		96 (4 per cell)
# of superperiods		24
Magnetic field at injection, B_0	(KGauss)	0.74
Magnetic field at extraction, B_0	(KGauss)	7
Bend magnet length	(m)	2.9
Circumference, Π	(m)	$2\pi \times 74.47$
Cycle time, T	(sec)	1/15

Beam parameters		
Transverse normalized emittance, $\epsilon_{x,y}$	(mm·rad)	12π
Longitudinal emittance, $\varepsilon_{\text{long}}$	(eV·sec)	0.25
Typical bunch intensity,		3×10^{10}
Injection kinetic energy, E_{kin}	(MeV)	400
Transition kinetic energy, E_{kin}	(GeV)	4.17
Extraction kinetic energy, E_{kin}	(GeV)	8

Appendix B. Head-tail modes experiment. Measured betatron tunes.

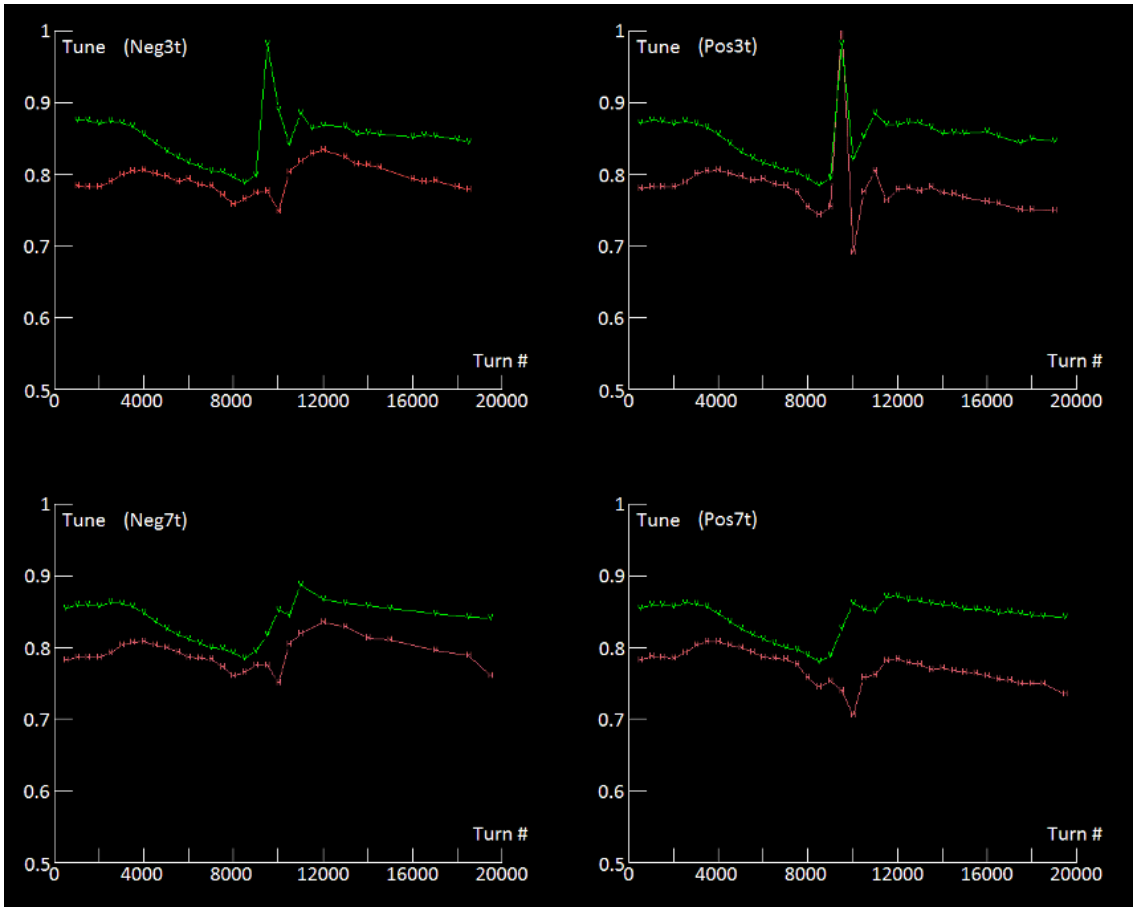

Red and green curves correspond to horizontal and vertical DOF.

Appendix C. Head-tail modes experiment. Measured chromaticity.

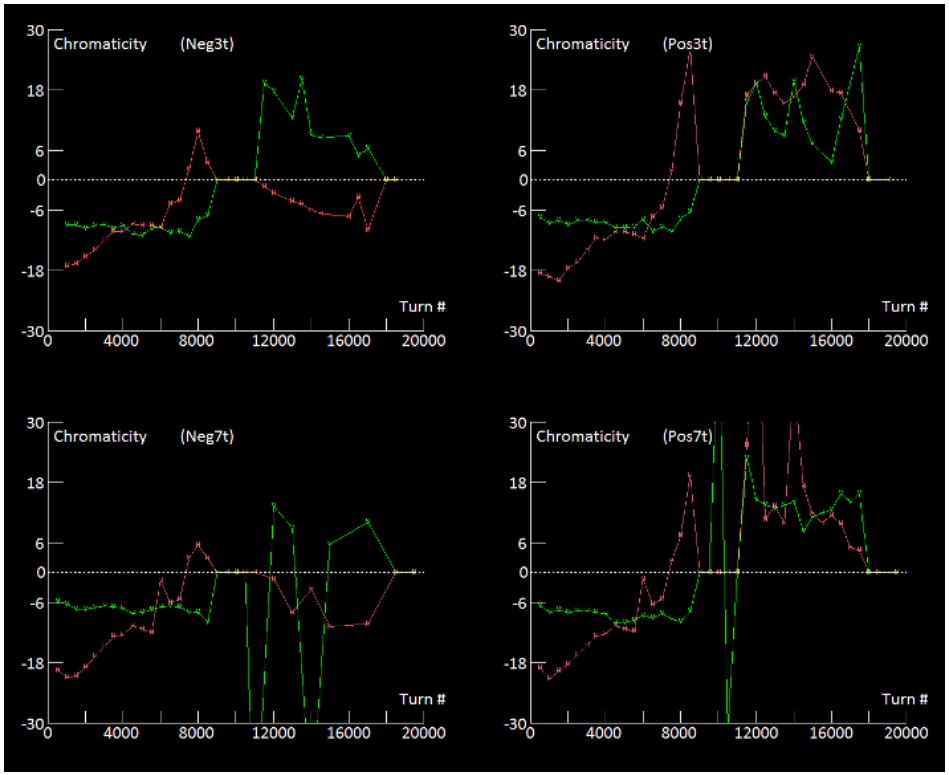

Data has been obtained for two settings of chromaticity: the post transition "normal" horizontal chromaticity about zero or a bit positive and post transition with negative horizontal chromaticity.